*Proceedings of the 7th European VLBI Network Symposium*
*Bachiller, R. Colomer, F., Desmurs, J.F., de Vicente, P. (eds.)*
*October 12th-15th 2004, Toledo, Spain*

# Methanol masers in environments of three massive protostars

A. Bartkiewicz ⋆[1], M. Szymczak[1], and H.J. van Langevelde[2]

[1] Toruń Centre for Astronomy, Nicolaus Copernicus University, Poland
[2] Joint Institute for VLBI in Europe, The Netherlands



**Abstract.** We present the first EVN maps of 6.7 GHz methanol masers of three high-mass protostar candidates selected from the Toruń unbiased survey of the Galactic plane. A variety of linear and arc like structures was detected. A number of maser clusters with projected sizes of 20−100 AU show monotonic velocity gradients. Some of them are roughly perpendicular to the major axes of these structures and can arise behind shock fronts.

## 1. Introduction

Observations of the 6668.519 MHz methanol maser transition, first detected by Menten (1991), appear to be powerful tools to identify the massive early type stars still embedded in their parental dense molecular clouds. The high brightness of this line enable us to investigate structures at milliarcsecond (mas) scales (a few hundreds of AU at the distances of a few kpc).

Phillips et al. (1998) analyzed 45 methanol maser sources in star-forming regions and divided them into five groups on the basis of their morphology: linear (curved), elongated, pair, complex and simple. The linear masers were outstanding in their survey and showed a monotonic or near-monotonic velocity gradient along the source major axis that is consistent with a model of masers embedded in a rotating disk (radius of a few thousands of AU) seen edge-on or nearly edge-on around a high mass (up to 120 $M_{\odot}$) protostar or OB star (Norris et al. 1998; Minier et al. 2000). However, Walsh et al. (1998) found only 12 sources showing velocity gradients in the sample of 97 methanol sites studied. They proposed a scenario in which the methanol masers appear before the UC H II phase around the protostar, associated with embedded non-ionizing stars. The dense knots of gas are compressed and accelerated by the passage of the shock and local conditions cause different geometries of maser spots. Dodson et al. (2004), based on the VLBI data, proposed that the 6.7 GHz methanol masers arise behind low-speed (<10 km s$^{-1}$) planar shock. A shock propagating nearly perpendicular to the line-of-sight produces a linear spatial distribution of maser components. Interaction of the shock with density perturbations in the star-forming region disrupts the linearity of maser structures.

The VLBI results presented below are first in a series for a large sample of methanol masers detected in the unbiased survey of the Galactic plane (Szymczak et al. 2002). Our aims are twofold; to investigate the mas scale of 6.7 GHz methanol maser structures in order to test the above mentioned hypotheses and to search for relationships of methanol emission with other tracers of star-forming activity. We improved the positions of newly detected 30 sources in the Toruń survey using the single baseline of MERLIN (Mark II and Cambridge antennas).

**Table 1.** Coordinates (J2000) of the target sources.

| Source | RA (h m s) | Dec ($^o$ ' " ) | ΔRA (") | ΔDec (") |
|---|---|---|---|---|
| G33.64−0.21 | 18 53 32.551 | 00 32 06.525 | 0.3 | 4 |
| G35.79−0.17 | 18 57 16.911 | 02 27 52.900 | 0.6 | 3 |
| G36.11+0.55 | 18 55 16.814 | 03 05 03.720 | 0.2 | 1.4 |

The absolute positions of the strongest maser features were determined with accuracies of 0.1−0.″8 in RA and 1−4″ in Dec depending on the source intensity and declination (Bartkiewicz et al., in prep.).

## 2. Observations and data reduction

The observations of methanol maser emission at 6668.519 MHz of the three star-forming regions G33.64−0.21, G35.79−0.17 and G36.11+0.55[1] were carried out with the European VLBI Network (EVN) on 2003 June 08. Useful data were obtained from four antennas (Cambridge, Effelsberg, Jodrell Bank and Onsala). In the single dish survey these sources showed complex methanol spectra with three of more clearly visible features of flux densities higher than 10 Jy. All of them are OH emitters (Szymczak & Gérard 2004). The coordinates of the target sources and their errors as measured with the Mark II − Cambridge baseline of MERLIN are given in Table 1.

The targets were observed for a total of 12 hr, together with observations of continuum source 3C345 for the purpose of bandpass, delay and rate calibration. The source J1907+0127 (0.2 Jy at 6.7 GHz) was used as a phase calibrator for all three targets. The cycle time between each target and the phase-calibrator was 5.5 min + 3.5 min. We used a spectral bandwidth of 2 MHz, resulting in the velocity coverage of 100 km s$^{-1}$, divided into 1024 channels at correlation to give a velocity resolution of 0.09 km s$^{-1}$. The bandwidth was centred at the local standard of rest (LSR) velocity of 65 km s$^{-1}$. Observations were made in left- and right-hand circular polarization, but since the methanol emission is not strongly circularly polarized both

⋆ formerly Niezurawska, e-mail: annan@astro.uni.torun.pl

[1] the names of sources follow their galactic coordinates

polarizations were averaged in order to improve the signal-to-noise ratio.

The data were correlated on the EVN Mk IV Data Processor operated by JIVE. We carried out the data reduction with standard procedures for spectra line observations using the Astronomical Image Processing System (AIPS). To make final maps we used 1 mas pixel separations and an elliptical restoring beam 14×6 mas with a PA of $-1^\circ$ and applied the uniform weighting. The rms noise level was of 7−10 mJy beam$^{-1}$ in emission-free Stokes *I* maps.

We created fringe rate maps of the brightest channels of the targets but still we failed to find the absolute position of our sources. The target sources were near zero declination (from $+0\overset{\circ}{.}5$ to $+3\overset{\circ}{.}1$). The phase-calibrator J1907+0127, the nearest one from the VLBA Calibrator Survey, was about 3° apart from all three targets. Furthermore, due to use of only four EVN telescopes listed above the uv-plane coverage was poor for N-S baselines. It is likely that these factors together with too long phase-referencing cycle time precluded a proper phase calibration. However, the positions of the strongest components of each target are known with accuracies better than $0\overset{''}{.}6$ in RA and 4″ in Dec (Table 1).

## 3. Results and Discussion

### 3.1. G33.64−0.21

Fig. 1 shows the spectrum and the overall distribution of maser emission in G33.64−0.21. The emission is seen in the velocity range from 58.5 to 63.3 km s$^{-1}$ and 94 maser components brighter than 40 mJy b$^{-1}$ (5$\sigma$) are detected. These form 12 clusters distributed along an arc like structure of overall size of about 150 mas that corresponds to 585 AU for the assumed near kinematic distance of 3.9 kpc. We do not note any regularity in the velocity of the whole structure that can be expected for a rotating disk. However, monotonic velocity gradients are found within six clusters named as A, C, F, G, J and K (Fig. 1). Angular sizes of individual clusters range from 5 to 18 mas i.e. their projected linear sizes range from 20 to 70 AU. We notice that for most clusters the velocity gradients are roughly perpendicular to the arc. We state, the methanol maser emission in G33.64−0.21 does not show large-scale velocity gradient but about half of the maser clusters exhibit internal velocity gradients some of which are roughly perpendicular to the arc. This can suggest that the maser structure forms in a shock front postulated by Dodson et al. (2004).

The inset in Fig. 1 shows that amplitude of feature L of the EVN spectrum is comparable (within 30%) with that of the single dish spectrum. For the rest of features the amplitudes observed with the EVN are a factor of 3-4 lower. This implies, even though variability and/or errors in flux density cannot be ruled out, that a large fraction of maser flux was missed in the interferometric observations. Therefore, G33.64−0.21 appears as a good candidate to map a low intensity and diffuse maser emission.

### 3.2. G35.79−0.17

The spectrum of G35.79−0.17 is composed of four features within the velocity range from 59.9 to 62.7 km s$^{-1}$ (Fig. 2). The shape of the spectrum is the same as observed in 2000 (Szymczak et al. 2002) but amplitude is about a factor of 2.5 lower. Variability of the source and calibration errors cannot fully account for such a difference. We suggest that there is diffuse emission missed during our EVN observations. We found the emission in 33 spectral channels and its distribution appears as a 9.5 mas linear structure (Fig. 2). Analysis of the position−velocity diagram revealed a linear velocity gradient along NE (red-shifted) – SW (blue-shifted) direction. Such a characteristic structure can arise from masers from an edge-on rotating disk or accelerating outflow. In a case of an edge-on rotating Keplerian disk we can estimate the lower limit of the mass of a central star (e.g. Phillips et al. 1998). Assuming the far and near kinematic distances of 4.6 kpc and 10.3 kpc we infer that the enclosed mass is 0.4 and 0.9 $M_\odot$, respectively. These values are certainly underestimated; we have assumed that there is no inclination and that the disk size equals the extension of the maser emission. Minier et al. (2000) found similar structures in W 51 and G 29.95−0.02. They also derived sub-solar masses and concluded from a larger sample that they had detected only a small fraction of the disk, which typically extends over 1000 AU. Indeed, the maser structure in G35.79−0.17 is similar in a size with individual clusters observed in G33.64−0.21 (e.g. the cluster A). We cannot exclude that the observed structure arises due to an outflow from a massive protostar signposted by infrared source IRAS18547+0223. Proper motion studies would help to solve the problem of origin of the linear structure of methanol maser in G35.79−0.17.

### 3.3. G36.11+0.55

Fig. 3 shows the spectrum and the distribution of the 6.7 GHz methanol maser emission in G36.11+0.55. We found two active regions, north-western and south-eastern separated by $1\overset{''}{.}1$. The maser components in both regions are elongated along a position angle of ∼45°. These structures are nearly perpendicular to the major axis. The NW region is composed of eight clusters, labelled from A to H, within the LSR velocity range from 81.1 to 84.5 km s$^{-1}$. The SE region is composed of six maser clusters, labelled from I to N, of the LSR velocity from 73.0 to 76.2 km s$^{-1}$. 4 out of 14 clusters exhibit monotonic velocity gradients; two of them (NW region) are perpendicular to the major axis. For the assumed near kinematic distance of 5.3 kpc the two clumps NW and SE are separated by 5840 AU.

The methanol emission of G36.11+0.55 lies $5\overset{''}{.}5$ SE from the centre of a giant molecular clump Mol 77 (IRAS18527+0301) with embedded high-mass protostars of type B2.5−O8.5 (Brand et al. 2001). Since the absolute position of methanol masers is known within $0\overset{''}{.}2$ and $1\overset{''}{.}4$ (RA and Dec) this positional offset may be significant. The velocities of thermal emission of CS, CO and $HCO^+$ range from 71.9 to 82.1 km s$^{-1}$ with the peaks about 75.5 km s$^{-1}$ and match well the velocity range of methanol emission. We note that the overall structure delineated by methanol masers is nearly

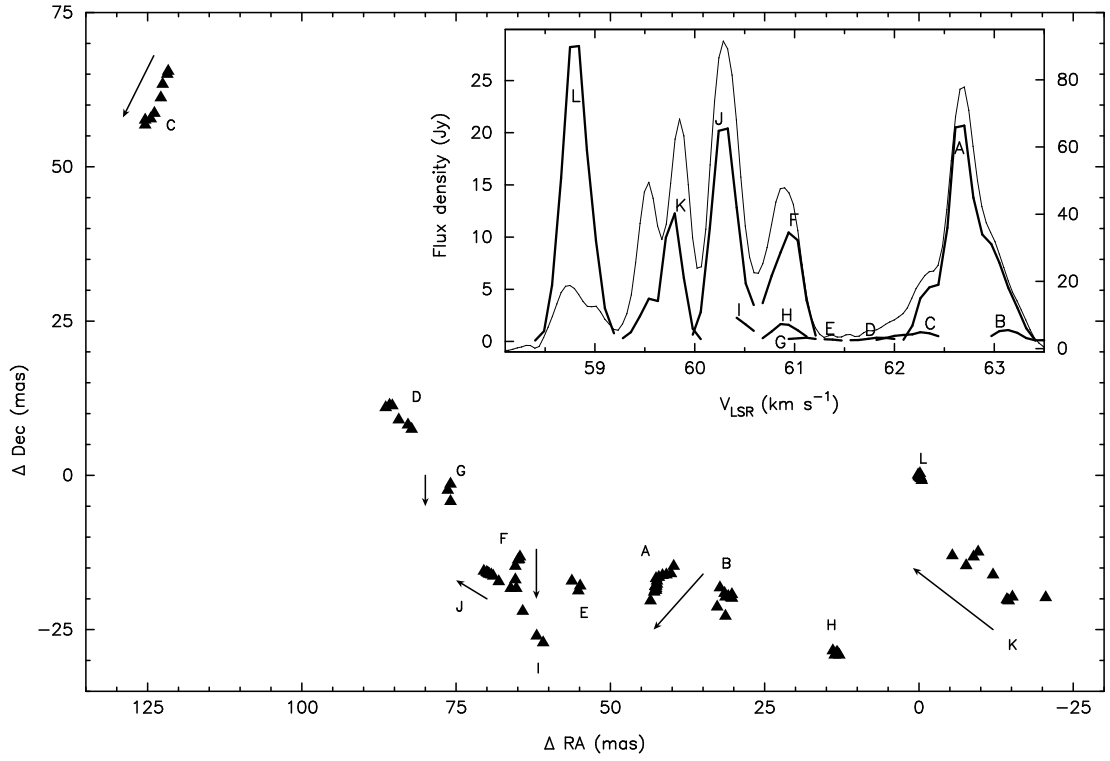


**Fig. 1.** The EVN 6.7 GHz methanol maser distribution in G33.64−0.21. The coordinates are relative to the strongest maser component (Table 1). Each triangle corresponds to a single component found in the channel maps. Maser clusters A, C, F, G, J and K show clear velocity gradients traced by arrows (pointed to the blue-shifted velocities). The spectrum (inset) is composed of emission profiles of maser clusters labelled from A to L. Thin line shows the single dish spectrum taken in 2000 and scaled with the right hand ordinate.

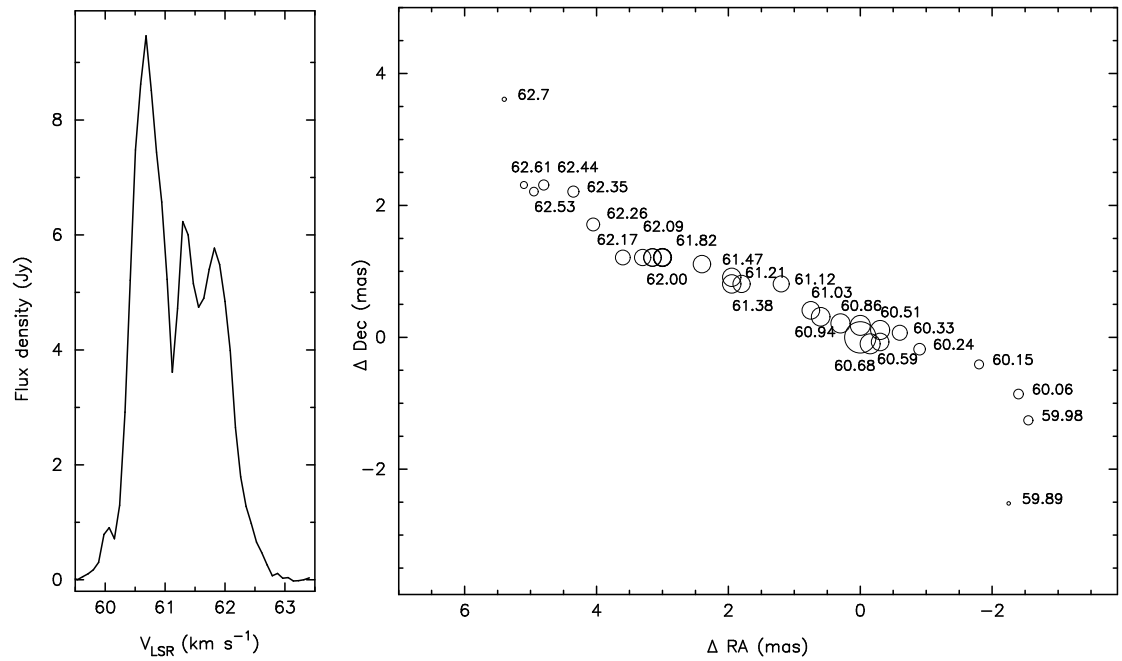


**Fig. 2.** The EVN 6.7 GHz methanol spectrum (left) and the distribution of maser components (right) in G35.79−0.17. The coordinates are relative to the brightest maser component (Table 1). Each circle corresponds to a single component found in the channel maps. The sizes of circles are proportional to the logarithm of the brightness. The numbers indicate the LSR velocities (km s$^{-1}$) of the components.

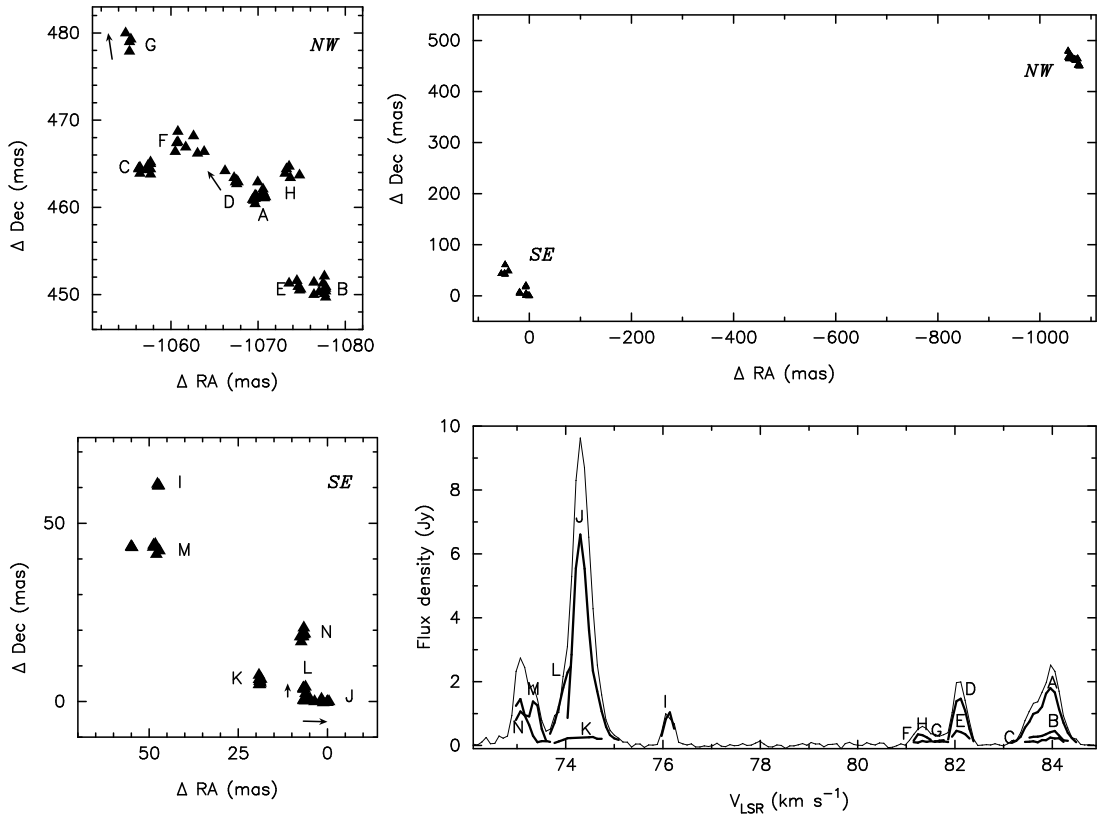


**Fig. 3.** The overall distribution (top right) and spectrum (bottom right) of the 6.7 GHz methanol maser emission in G36.11+0.55. The coordinates are relative to the strongest maser component (Table 1). Enlarged areas of the NW and SE emission are shown on the left side. Each triangle corresponds to a maser component found in the channel maps. Arrows mark velocity gradients similarly as in Fig. 1. The spectrum shown by thin line is the sum of spectra of individual maser clusters (thick line).

perpendicular to the axis of an outflow traced by the blue- ($71.0-73.8\,\mathrm{km\,s^{-1}}$) and red-shifted ($79.5-83.2\,\mathrm{km\,s^{-1}}$) emission of the $^{13}$CO line as reported by Brand et al. (2001). Therefore it is very likely that the 6.7 GHz maser emission mapped with the EVN are physically related to a high mass protostar.

## 4. Conclusions

The 6.7 GHz methanol maser emission towards three star-forming regions was imaged with milliarcsecond resolution. Linear and arc like structures were detected. There were considerable numbers of maser clusters with internal velocity gradients roughly perpendicular to the major axis. These geometrical structures can arise in outflows and behind shock fronts.

*Acknowledgements.* AB acknowledges the support from JIVE during her stay in Dwingeloo. The European VLBI Network is a joint facility of European, Chinese, South African and other radio astronomy institutes funded by their national research councils. The work was supported by the KBN grant 2P03D01122.

## References

Brand, J., Cesaroni, R., Palla, F., & Molinari, S. 2001, A&A 370, 230
Dodson, R., Ojha, R., & Ellingsen, S.P. 2004, MNRAS 351, 779
Menten, K.M. 1991, ApJ, 380, L75
Minier, V., Booth, R.S., & Conway, J.E. 2000, A&A, 362, 1093
Norris, R.P., Byleveld, S.E., Diamond, P.J., et al. 1998, ApJ, 508, 275
Phillips, C.J., Norris, R.P., Ellingsen, S.P., & McCulloch, P.M. 1998, MNRAS, 300, 1131
Szymczak, M., Kus, A.J., Hrynek, G., Kepa, A., & Pazderski, E. 2002 ,A&A, 392, 277
Szymczak, M., & Gérard, E. 2004, A&A, 414, 235
Walsh, A.J., Burton, M.G., Hyland, A.R., & Robinson, G. 1998, MNRAS, 301, 640